Estimation of the characteristic times of solvent diffusion and polymer relaxation in glassy polymer films by a set inversion method

Frédéric Doumenc, B. Guerrier

Inverse Problems in Science and Engineering
Vol. , No. , , 1–26

Estimation of the characteristic times of solvent diffusion and polymer relaxation in glassy polymer films by a set inversion method

F. DOUMENC* and B. GUERRIER
Université Pierre et Marie Curie-Paris 6, UMR 7608, Orsay, F-91405 France ;
CNRS, UMR 7608, Orsay, F-91405 France ;
Laboratoire FAST, Bât. 502, Campus Universitaire, 91405 Orsay, France
()

This study deals with a multi parameter estimation problem with bounded output errors. It concerns the swelling of polymer films by a solvent, in the glassy state. Local thermodynamic equilibrium is no more ensured and the swelling results of two coupled phenomena, the diffusion of solvent on one hand and the change in solubility due to stress relaxation of the entangled polymer chains on the other hand. The estimation aims to obtain the parameters that characterise these two phenomena from gravimetric experiments. A set inversion analysis is used to perform the estimation: this global estimation method allows to determine all the sets of parameters that give a mass uptake consistent with the experimental data and the bounded errors. It gives interesting information on the coupling between the parameters and is well appropriate to analyse this ill-conditioned problem. A systematic analysis of the estimation performance as a function of the characteristics of the polymer/solvent system and of the experimental set-up have been performed.

1 Introduction

Diffusion of solvents or low molecular weight species in polymer films or membranes is the determining factor in many processes such as the drying of polymer coatings, membrane formation, drug release, etc. When the polymer film is rubbery, i.e. when its temperature is well above the glass transition temperature, solvent sorption (swelling) or desorption (drying) is well known. Swelling or drying kinetics is much more complex in the glassy domain: indeed local thermodynamic equilibrium is no more ensured since the relaxation of the stresses induced by the volume variations involves rearrangements of macromolecular chains which are very slow and may be longer than the characteristic time of diffusion. The swelling of a polymer film then results of two coupled

Corresponding author; E-mail: doumenc@ccr.jussieu.fr; Fax: +33 1 69 15 80 60; Tel: +33 1 69 15 80 63

phenomena, the diffusion of solvent on one hand and the change in solubility due to stress relaxation on the other hand [1–5].

One common way to investigate solvent sorption is to perform gravimetry experiments in a controlled environment: The film is swelled by small increasing of the solvent vapor pressure above the film and the evolution of the film mass induced by the variation of the vapor pressure is recorded. In the same way, desorption experiments are obtained by performing small decreasing steps of the solvent vapor pressure above the film. One example of desorption kinetics, for a copolymer PMMA/PnBMA (polymethylmethacrylate/polynbutylmethacrylate) swelled by toluene, is given in figure 1 [6]. If the film were not glassy, the kinetics due to a small pressure step should exhibit a Fickian behaviour: the absolute value of the mass variation as a function of the square root of time should be linear at the beginning and should go to an asymptotic value [7]. The deviation from Fickian behaviour is typical of the glassy state. In this example 'pseudo Fickian' kinetics is obtained with a linear part at short times followed by a slow increase of the absolute value of the film mass variation. More complex kinetics can be obtained (S shaped curves or non monotonic mass variations for example) depending on the coupling between diffusion and relaxation [8].

One important point to underline is that experimental errors in such devices may be badly characterised: for example in quartz microbalance set-up, besides the usual measurement noise that can be statistically modeled, one can observe drifts or systematic errors due to pressure or temperature influence on the quartz behaviour [5, 6, 9]. These errors are not accurately known and can only be bounded. The estimation problem is then the following: given the experimental mass evolution and some bounds on the experimental errors, is it possible to estimate the parameters that characterise solvent sorption in the glassy state? More generally this study is part of the problem of multi parameter estimation with bounded experimental errors.

Classical optimization methods based on the minimization of the distance between experimental and modeled kinetics are not suitable for such an estimation problem. Indeed the minimization selects one solution in the parameter space and estimates the uncertainty from the errors statistical laws. As seen later, the estimation problem considered here is badly conditioned in the sense that very different set of parameters give close kinetics. Then the selection of one solution is meaningless, especially as the uncertainty cannot be easily determined since measurement errors are only bounded. That is why another estimation approach has been chosen, a set inversion analysis: this global estimation method aims to determine all the sets of parameters that give a kinetics consistent with the experimental data and the bounded errors [10–13]. This kind of approach is very interesting because it gives well defined error intervals for each parameter. Then, for a given experimental situation, it is possible to

determine if the different parameters are accurately or only roughly estimated. Let us note that the diffusion coefficient and the relaxation time vary on several decades in the glassy domain [8, 14]. Then, getting at least the order of magnitude of these parameters is an interesting information.

The paper is organised as follows: the physical model used to simulate sorption in glassy films is presented in section 2. Section 3 is devoted to a brief presentation of the set inversion method. The performance of the estimation as a function of the coupling level between diffusion and relaxation is analysed in section 4.

2 Sorption modeling

The glassy state is not well understood yet and several theoretical approaches have been proposed to model solvent sorption in glassy films, none of them succeeding in fitting all the observed behaviours. One of these approaches takes viscoelastic relaxation into account through a constitutive equation, where the relaxation behavior is approximated by a simple viscoelastic model [1–3, 15]. A second group of models takes the coupling between diffusion and relaxation into account through the solubility (time dependent solubility model [4, 16–20]).

In the absence of a well defined description of the glassy state, we opted for a phenomenological model of the literature, simple enough to be suitable for the estimation algorithm used in this study, but able to capture the main features of sorption swelling. In the model proposed by Long and Richman [16] the relaxation is taken into account at the interface only: each volume element in the bulk is assumed to be at the local thermodynamical equilibrium and the classical formulation for Fickian diffusion is employed to describe the solvent diffusion through the film. In gravimetry experiments considered here, the film swelling is obtained by increasing the solvent vapor pressure in the measurement chamber. For each experiment the vapor pressure variation is very small so that the solvent uptake is very small too and the diffusion coefficient and film thickness can be assumed constant during one experiment:

$$\frac{\partial c(z,t)}{\partial t} = D_{sp}\frac{\partial^2 c(z,t)}{\partial z^2}, \quad 0 < z < l \tag{1}$$

where $c(z,t)$ is the local solvent concentration, D_{sp} is the mutual diffusion coefficient and l is the film thickness.

The solvent vapor is the only gas in the measurement chamber so that changing the vapor pressure leads to a change of the surface concentration (first kind boundary condition). In the Long and Richman model [16], the

effect of the relaxation is introduced by making the surface concentration a function of time with a first order model. Then, assuming a perfect pressure step of the vapor above the film, the boundary condition at the film/vapor interface is given by:

$$c(z = l, t > 0) = c_0 + (c_\infty - c_0) \left\{ 1 - exp\left(-\frac{t}{\tau_r} \right) \right\} \tag{2}$$

where c_0 is the instantaneous change of the surface solvent concentration after a pressure step, c_∞ is the equilibrium value corresponding to the thermodynamical equilibrium and τ_r is the relaxation characteristic time. Let us notice that, in the rubbery domain, the rearrangement of macromolecular chains is very rapid ($\tau_r \simeq 0$) and equation (2) amounts to a constant first kind boundary condition, as expected when no inert gas is present. The second term in equation (2) expresses the slow evolution of the solubility due to the slow relaxation of stresses in the glassy state.

The boundary condition at the bottom of the film is a condition of non permeability:

$$\frac{\partial c}{\partial z}(z = 0, t) = 0 \tag{3}$$

The initial condition is:

$$c(z, t = 0) = c_i \tag{4}$$

To simplify the notations, the initial concentration, c_i, is always set to zero in the following. This shift of the concentration has no impact on the model behaviour since equations are linear. The mass uptake by unit area, Δm (Kg/m^2), is noted m in the following.

This model is of course an approximation since, among other things, it assumes thermodynamical equilibrium inside the film and uses a first order model to represent relaxation. But it was shown to be able to fit experimental kinetics. Moreover a systematic comparison with the model proposed by Petropoulos [21], in which the relaxation is taken into account everywhere in the film, was performed. This comparison showed an agreement good enough for estimation purpose [22]. From the numerical point of view, the Long and Richman model is simpler because the relaxation is introduced through a boundary condition only and not in the equation describing solvent diffusion inside the film.

Four parameters (τ_r, τ_d, c_0 and c_∞) and two dimensionless quantities are involved in this model: the Deborah number compares the characteristic times of diffusion and relaxation: $Deb = \tau_r/\tau_d$, with $\tau_d = l^2/D_{sp}$; R is the ratio

between the instantaneous and delayed component of the solvent concentration uptake: $R = c_0/c_\infty$. A very small Deb corresponds to the rubbery Fickian case, when relaxation phenomena are instantaneous on the diffusion time scale so that the system is in local thermodynamic equilibrium. On the contrary a very large Deborah leads to two stages kinetics (the two phenomena are well separated) or even to Fickian kinetics if the second stage is not observed on the time scale of the experiment. More complex kinetics is obtained for intermediate values depending on both Deb and R, as illustrated on figure 2.

An analytic expression of the solvent mass uptake $m(t)$ can be derived from the above equations by use of Laplace transforms [6]:

$$m^*(t) \;=\; 1 - tan\left(\frac{1}{\sqrt{Deb}}\right)\sqrt{Deb}\;(1-R)\;exp\left(-\frac{t^*}{Deb}\right) + 2\sum_{k'=\frac{\pi}{2}}^{\infty}\left(\left[\frac{\frac{1}{Deb} - Rk'^2}{k'^2\left(k'^2 - \frac{1}{Deb}\right)}\right]\;exp(-k'^2 t^*)\right) \tag{5}$$

with: $k' = (2k+1)\frac{\pi}{2}$, $\quad m^*(t) = m(t)/m_\infty$, $\quad m_\infty = c_\infty \times l$, $\quad t^* = \frac{D_{sp}t}{l^2} = \frac{t}{\tau_d}$.

As illustrated in the following, one of the difficulties of this multi parameter estimation problem arises from the quite similar form of the terms of equation (5): this is due to the expression of the solution of the diffusion equation, which is an infinite sum of decreasing exponentials, and the relaxation model which is a decreasing exponential. The numerical tests described in section 4 analyse the performance of the estimation of the four parameters (τ_r, τ_d, $m_0 = c_0 \times l$ and R) as a function of Deb, R, the duration of the experiment H and the measurement error level σ.

3 Set inversion analysis

3.1 *Method*

This section gives a brief presentation of the global optimization method, applied to the estimation problem considered in this paper. A more general presentation and rigorous demonstrations of the mathematical properties can be found in [10–13]. As said previously, the set inversion analysis aims to characterize the set of all the values of the parameters that are consistent with the data in the sense that the differences between the experimental data and model outputs fall within prior bounds.

A key stage in the set inversion analysis is the definition of the bounded errors. These errors are defined a priori, i.e. before the estimation, and must take into account all the uncertainties of the experimental set-up. One example of errors definition in the case of a gravimetry set-up based on a quartz microbalance can be found in [5]. In the analysis performed here we have chosen to simulate experimental errors by a constant value, σ, since a detailed

description of σ strongly depends on the experimental set-up. (However let us note that using a non constant σ is straightforward). That means that at each experiment time t_k, the true mass is assumed to lie between $(m^k_{exp} - \sigma)$ and $(m^k_{exp} + \sigma)$ where m^k_{exp} is the measured mass at t_k. Then we are interested to find all the quadruplets $\mathbf{p} = \{\tau_d,\, \tau_r,\, m_0 = c_0 \times l,\, R\}$ for which the output of the model $m(t = t_k)$ (c.f. equation (5)) lies between $(m^k_{exp} - \sigma)$ and $(m^k_{exp} + \sigma)$ at all measurement times t_k.

First we introduce some definitions used in the set inversion analysis. Considering a given quadruplet $\mathbf{p} = \{\tau_d,\, \tau_r,\, m_0,\, R\}$ and the corresponding model output $m(\mathbf{p}, t)$, $\mathbf{p}$ is said admissible if:

$$\forall k \in \mathrm{N} \mid 1 \leq k \leq n, \quad (m^k_{exp} - \sigma) \leq m(\mathbf{p}, t_k) \leq (m^k_{exp} + \sigma) \tag{6}$$

with n the number of measurements, $m(\mathbf{p}, t_k)$ the model output at t_k obtained with the quadruplet $\mathbf{p}$.

If for some times t_k the distance between the model output and the data is greater than σ, the quadruplet is rejected and said non admissible:

$$\exists k \in \mathrm{N} \mid 1 \leq k \leq n, \quad m(\mathbf{p}, t_k) < (m^k_{exp} - \sigma) \quad \text{or} \quad m(\mathbf{p}, t_k) > (m^k_{exp} + \sigma) \tag{7}$$

In the parameter space (dim=4), a box P is defined by the following inequalities:

$$\begin{aligned} \tau_{d_{min}} \leq\ & \tau_d \leq \tau_{d_{max}} \\ \tau_{r_{min}} \leq\ & \tau_r \leq \tau_{r_{max}} \\ m_{0_{min}} \leq\ & m_0 \leq m_{0_{max}} \\ R_{min} \leq\ & R \leq R_{max} \end{aligned}$$

A box is said admissible if all the quadruplets contained in the box are admissible, and on the contrary non admissible if all the quadruplets of the box are non admissible. A box that contains admissible and non admissible quadruplets is said ambiguous. At least, a box that cannot be put in one of these three categories due to incomplete information is said indeterminate. Indeed, as will be seen later, usually only sufficient conditions of admissibility are available. When these conditions are not fulfilled, the box is indeterminate.

It is of course not possible to perform this classification directly because each box contains an infinite number of quadruplets. The image of the box, $m(\mathrm{P}, t)$, is the set of the outputs of the model for all the quadruplets of the box. It is generally difficult to obtain this image directly. To obtain the partition of the parameters space into the admissible domain and the non admissible

one, the authors of set inversion methods introduce the notion of inclusion function. Details are given in [11, 13]. Qualitatively it can be introduced in the following way: the inclusion function M is used to determine an including envelope for the images of the boxes: $M(\mathrm{P}, t)$ must include the image of the box, $m(\mathrm{P}, t)$, and its size must go to zero if the size of the box P goes to zero. The determination of an inclusion function is a key preliminary step in the set inversion analysis. A schematic illustration of an inclusion function is given in figure 3 for a simple example where the dimension of the parameter space as well as the dimension of the image space are two [11]. (This would correspond to the estimation of 2 parameters, for example τ_d and τ_r, using the mass measurement at only two times, t_1 and t_2).

In the problem considered here, the image of a box can be quite easily bounded. Indeed, when $R < 1$, the model output is a monotonic function of the four parameters τ_d, τ_r, m_0 and R: it is an increasing function of m_0 and a decreasing function of τ_d, τ_r and R (cf. Appendix A). The model output for any quadruplet of the box is then included between the kinetics obtained by the quadruplets $\mathbf{p_{low}} = \{\tau_{d_{max}}, \tau_{r_{max}}, m_{0_{min}}, R_{max}\}$ and $\mathbf{p_{up}} = \{\tau_{d_{min}}, \tau_{r_{min}}, m_{0_{max}}, R_{min}\}$.

The case $R > 1$ is a little more complex but it is also possible to define two quadruplets $\mathbf{p_{low}}$ and $\mathbf{p_{up}}$ and two bounds, m_{low} and m_{up} including the image of the box, as detailed in Appendix A.

Then the partition of the boxes can be made in the following way: For a box P to be admissible, it is sufficient that the two extreme quadruplets are admissible. On the contrary, if for at least one time t_k the output m_{low} is greater than $(m^k_{exp} + \sigma)$ or the output m_{up} is smaller than $(m^k_{exp} - \sigma)$, the box is non admissible. Otherwise it is indeterminate. Indeed the two previous conditions are sufficient but not necessary.

3.2 *Algorithm SIVIA ("Set Inversion Via Interval Analysis")*

Once the inclusion function is obtained, the numerical algorithm is quite simple to implement. SIVIA uses a stack of boxes [11, 13]. First an initial box in the parameter space, large enough to contain all the possible solutions, is specified. This initial box, P_0, is indeterminate. The required accuracy for the final paving, ε, is also specified. This box is put on top of the stack and bisect into two smaller boxes. Each sub-box is tested by computing m_{low} and m_{up}. An admissible sub-box is stored in the 'solution file', a non admissible box is deleted and an indeterminate one is put on top of the stack, if its size is greater than ε. If not, it is stored in the 'indeterminate file'. Then the procedure is repeated till the stack is empty. Convergence properties of the algorithm are analysed in [13].

At the end of the calculation, one obtains the domain in the parameter

space containing the admissible quadruplets, K_A, and the frontier between the admissible and non admissible domains corresponding to the indeterminate boxes, K_I. The solution of the estimation problem is made of the union of the two domains, $(\mathrm{K}_A \cup \mathrm{K}_I)$. The thickness of the indeterminate domain depends on ε, so that decreasing ε decreases the size of K_I. But on the other hand the computing time is very sensitive to ε and the choice of ε then is a compromise. For each of the four parameters $\mathbf{p} = \{\tau_d, \tau_r, m_0, R\}$, the 1D projection of the solution on the four axes of the parameter domain gives all the values that are consistent with the experimental kinetics and the bounded errors. Of course all the combinations are not possible and the projections of the solutions in 3 or 2 dimensions give interesting information on the coupling between the parameters.

As other non linear optimisation algorithm, SIVIA requires the calculation of $m(t)$ a great amount of times so that it is computer time consuming, though the calculus of the output $m(t)$ itself is very rapid. But it can be very easily parallelized because the boxes on the stack can be analysed independently (cf. numerical subsection in the following). Let us recall that, despite the great computing time required by SIVIA, the advantage of this global optimization method is to give all the sets of parameters that give a kinetics consistent with the experimental data and the bounded errors, while a classical optimisation method would select only one solution.

4 Estimation results

The tests of the estimation method have been performed in the following way: For a given set of parameters, $\mathbf{p}^{ref} = \{\tau_d^{ref}, \tau_r^{ref}, m_0^{ref}, R^{ref}\}$, the output is calculated for $0 \leq t \leq H$. Then this output is used as experimental kinetics, m_{exp}. The SIVIA algorithm is then performed to determine all the quadruplets $\mathbf{p} = \{\tau_d, \tau_r, m_0, R\}$ that give kinetics $m(t)$ such that $(m_{exp}^k - \sigma) < m(t_k) < (m_{exp}^k + \sigma)$.

The diffusion time τ_d^{ref} and the mass at equilibrium, m_∞^{ref}, are set to one in all the simulations. The time sampling, $t_{k+1} - t_k$, is very small compared to the two characteristic times τ_d and τ_r. We have studied the influence of Deb, R, the experiment duration H and the error level σ on the estimation performance.

4.1 *Influence of Deb*

In a first step the error level is set to 0.01, that is 1% of the mass variation at equilibrium. The duration H is large compared to the characteristic times τ_d

and τ_r.

Let us first analyse the influence of the Deborah number for a given R value: R^{ref} is set to 0.5 (the instantaneous change of the concentration at the interface film/vapor is half the total variation) and tests are performed for $Deb^{ref} = \tau_r^{ref}/\tau_d^{ref}$ from 0.1 to 100.

1D projections for the four parameters are given in figure 4. The representation is given for τ_d, τ_r, R and $m_\infty = m_0/R$. Vertical bars correspond to the values of the parameters that are consistent with experimental data, corresponding to $(\mathrm{K}_A \cup \mathrm{K}_I)$. Let us note that in all the results presented in the paper ε (the required accuracy for the final paving) is small, so that the frontier K_I is thin. Figure 4 shows that the quality of the estimation strongly depends of the Deborah number. For Deb greater than about three estimation with good accuracy is obtained for the four parameters. For small Deborah the parameters may vary on large intervals, except for the mass at equilibrium which is always obtained with a good accuracy because the experiment duration H is large. Indeed, the mass variation induced by diffusion and relaxation can be simulated by a great number of parameter combinations. As said previously, this is due to the quite similar form of the solution of the diffusion equation, and the relaxation term. The kinetics can then be obtained numerically by several parameters sets if Deb is close to one, when the two phenomena are strongly coupled, or if Deb is small, when the kinetics is not sensitive to relaxation in the real problem. Figure 5 gives an illustration of the ill conditioned character of the estimation problem for small Deb: kinetics are very close with quite different parameters. On the contrary for Deb greater than three diffusion and relaxation are less coupled and the shape of the kinetics depends on the two phenomena sufficiently to get small variation domains for the four parameters.

This is confirmed by the observation of 2D projections (figure 6). The size of the admissible domain in the 'τ_r/Deb^{ref}, τ_d' space increases when Deb decreases. In the 'm_0,R' space the admissible domain is close to the bisectrix because the equilibrium value is accurately estimated. But the length of the domain increases when Deb decreases.

These first tests show the advantage of this global optimization method to thoroughly characterise the accuracy of the estimation. Let us notice that, in such a situation, estimation performance improvement is possible by decreasing the film thickness. Indeed the diffusion time varies as the square of the film thickness while the relaxation time does not depend on it. As long as it is compatible with the specificity of the gravimetric set-up (sensitivity, minimal sampling times...), it is possible to choose experimental conditions suitable for accurate estimation.

4.2 *Influence of R*

To study the influence of R we now use a great Deb number, $Deb^{ref} = 10$. Tests have been performed for R^{ref} from 0 to 1.9. As previously the error level is set to 0.01 and the experiment duration H is large compared to the characteristic times τ_d and τ_r. 1D projections are given in figure 7 as a function of R. There are two critical zones, when R is small and when R is close to one. This may be explained when looking at equation (2). When $R = 1$, $c_0 = c_\infty$ and the instantaneous change in the boundary condition is equal to the equilibrium value, i.e. the stress relaxation does not induce a delayed swelling of the film. Then the relaxation term in the boundary condition disappears and the estimation of τ_r is no more possible. As shown in the previous section, the similar form of the diffusion equation solution and the relaxation model implies that numerically a great number of parameters combinations are able to give kinetics in the error bounds. Then none of the parameters except m_∞ are accurately estimated.
The second critical domain, $R < 0.3$, corresponds to a situation where the major part of the film swelling is due to the slow delayed component due to relaxation. As can be seen on the τ_r and R 1D projections, the solution for $R < 0.3$ is composed of two disconnected domains which corresponds to two families of solutions, the mass uptake being numerically ensured in major part by diffusion or relaxation. The estimation performance is good for $0.3 < R < 0.8$.
$R > 1$ corresponds to overshoot kinetics (cf figure 2): the mass uptake due to diffusion at the beginning of the experiment decreases later, due to the long time behavior of the sample [23, 24]. When R is greater than about 1.2, the delayed swelling is large enough to ensure accurate estimation of the four parameters.

Unlike for the Deborah number that can be increased by decreasing the film thickness, R cannot be changed for a given sample. These results highlights the bad conditioning of this estimation problem and the great care needed when analysing gravimetric experiments.

4.3 *Influence of H and σ*

To complete the characterization of this estimation problem, we have analysed the influence of the experiment duration H that may be an important limiting factor. Indeed relaxation time in polymer systems may be very long and it may be not possible to extend the experiment till the equilibrium mass is reached. For the test case $Deb^{ref} = 10$ and $R^{ref} = 0.5$, the influence of the experiment duration is given in figure 8, for H varying from 1 to 1000. As can be seen, a duration at least two times the relaxation time is needed to get accurate

results. If not, the obtained results once again show that close kinetics may be obtained by very different sets of parameters.

The last point concerns the influence of the error level σ. Tests were performed with $Deb^{ref} = 10$, $R^{ref} = 0.5$, a large experiment duration, and σ from 0.001 to 0.1. The performance of the estimation decreases strongly when the error level reaches 0.1 as shown in figure 9.

4.4 *Numerical*

The computations were performed with a PC Pentium IV on one hand and with an IBM RS6000 (eight processors by node - Centre de Calcul Recherche et Enseignement of the University Pierre et Marie Curie-Paris6) on the other hand. The computing time strongly depends on ε, the required accuracy of the final paving. For the test case $Deb = 10$, $R = 0.5$, $\sigma = 0.01$ and $H = 100$ and for a mono-processor computer (Pentium IV 3GHz), table 1 and figure 10 shows the influence of ε on the CPU and on the partition of the admissible and indeterminate domains. ε is defined relatively to the initial box. The algorithm is stopped when the size of all the indeterminate boxes is smaller than ε in the four directions of the parameter space. Let us note that the calculation of the model output itself, $m(t)$, is very rapid, about 100 ms. The initial box was the following:

$$\begin{aligned} 0.1 \leq\ & \tau_d \leq 10 \\ 1 \leq\ & \tau_r \leq 100 \\ 0.1 \leq\ & m_0 \leq 1 \\ 0.1 \leq\ & R \leq 1 \end{aligned}$$

The algorithm rapidly succeeds to estimate the order of magnitude of the parameters: 33 s are needed for $\varepsilon = 8 \times 10^{-3}$. Even if no admissible domain is obtained, the indeterminate domain is much smaller than the initial box. Increasing the accuracy of the solution is time consuming: almost one hour is needed with $\varepsilon = 10^{-3}$, that already gives a well defined solution domain, and about eight hours with $\varepsilon = 5 \times 10^{-4}$.

This numerical comparison was made on a well-conditioned test case. The CPU also strongly depends on the more or less ill conditioned character of the problem and may increases up to 100 hours, with Deb smaller than one or R close to one for example.

With such an algorithm the parallelization is very efficient, because the boxes can be analyse independently. With an eight processors computer (RS 6000, OpenMP library) the CPU times is divided by about seven compared to the

Table 1. Numerical comparison: paving accuracy (ε), CPU, ratio of the volume of the admissible domain on the volume of the admissible plus indeterminate domain ($V_{\mathbb{K}_A}/(V_{\mathbb{K}_A} + V_{\mathbb{K}_I})$).

ε	CPU	$V_{\mathbb{K}_A}/(V_{\mathbb{K}_A} + V_{\mathbb{K}_I})$
8×10^{-3}	33s	0
4×10^{-3}	112s	0.0019
2×10^{-3}	528s	0.08
1×10^{-3}	1h 6mn	0.283
5×10^{-4}	7h 25mn	0.529

non parallelized version.

5 Conclusion

A set inversion analysis has been used for the estimation of the four parameters involved in the swelling of polymer films: the characteristic times of diffusion and relaxation and the instantaneous and delayed components of the solubility. This global optimization method is very interesting in such a multi parameter estimation problems with bounded errors. Indeed it gives an overview of the domain where the estimation would lead to accurate results, the domain where only the order of magnitude of the parameters would be obtained and the domain where the problem is too ill conditioned to allow a meaningful estimation. Qualitatively, in the problem presented here, accurate estimation is possible only if the two phenomena are both observable on the kinetics. If not (Deb or R close to one or very small, H too small ...), the size of the admissible domain increases very rapidly. This study highlights the difficulty of gravimetric experiments interpretation in the glassy state, due to the coupling between relaxation and diffusion. In the present study the analysis was limited to the influence of experimental errors. As an improvement, it would be interesting to take into account the modeling errors due to the simplifying assumptions used in the model, as far as is it possible to estimate a bound of this modeling errors.

Acknowledgments

The numerical calculations have been partly performed on the computers of the 'Centre de Calcul Recherche et Enseignement' of the University Pierre et Marie Curie-Paris6.

References

[1] Thomas, N. and Windle, A., 1982. A theory of case II diffusion. *Polymer*, **23** 529–542.
[2] Durning, C., 1985. Differential sorption in viscoelastic fluids. *J. Polym. Sci.*, **23** 1831–1855.
[3] Edwards, D. and Cohen, D., 1995. A mathematical model for a dissolving polymer. *AIChE J.*, **41** 2345–2355.

[4] Sanopoulou, M., Stamatialis, D. and Petropoulos, J., 2002. Investigation of case ii diffusion behaviour. 1. theoretical studies based on the relaxation dependent solubility model. *Macromolecules*, **35** 1012–1020.
[5] Dubreuil, A.-C., Doumenc, F., Guerrier, B., Johannsmann, D. and Allain, C., 2003. Analysis of the solvent diffusion in glassy polymers using a set inversion method. *Polymer*, **44** 377–387.
[6] Saby-Dubreuil, A.-C., 2001. Séchage de films polymères : Etude du couplage entre la diffusion et la transition vitreuse - application à des copolymères pmma/pnbma. Ph.D. thesis, de l'université Paris VI.
[7] Doumenc, F., Guerrier, B. and Allain, C., 2005. Coupling between mass diffusion and film temperature evolution in gravimetric experiments. *Polymer*, **46** 3708–3719.
[8] Sanopoulou, M. and Boom, J., 2000. Interval sorption kinetics in the system poly(methyl methacrylate)-methyl acetate. *Polymer*, **41** 8641–8648.
[9] Bouchard, C., Guerrier, B., Allain, C., Laschitsch, A., Saby, A.-C. and Johannsmann, D., 1998. Drying of glassy polymer varnishes: A quartz resonator study. *J. Appl. Polym. Sci.*, **69** 2235–2246.
[10] Moore, R., 1992. Parameter sets for bounded-error data. *Mathematics and Computers in Simulation*, **34** 113–119.
[11] Walter, E. and Pronzato, L., 1997. *Identification of parametric models from experimental data* (Springer-Verlag, London).
[12] Jaulin, L. and Walter, E., 1993. Guaranteed nonlinear parameter estimation from bounded-error data via interval analysis. *Mathematics and Computers in Simulation*, **35** 123–137.
[13] Jaulin, L. and Walter, E., 1993. Set inversion via interval analysis for nonlinear bounded-error estimation. *Automatica*, **29(4)** 1053–1064.
[14] Dubreuil, A.-C., Doumenc, F., Guerrier, B. and Allain, C., 2003. Mutual diffusion in pmma/pnbma copolymer films - influence of the solvent induced glass transition. *Macromolecules*, **36** 5157–5164.
[15] Witelski, T., 1996. Traveling wave solutions for case II diffusion in polymers. *J. Polym. Sci. B*, **34** 141–150.
[16] Long, F. and Richman, D., 1960. Concentration gradients for diffusion of vapors in glassy polymers and their relation to time dependent diffusion phenomena. *J. Am. Chem. Soc.*, **82** 513–519.
[17] Frisch, H. L., 1964. Isothermal diffusion in systems with glasslike transitions. *J. Chem. Phys.*, **41(12)** 3679–3683.
[18] Berens, A. and Hopfenberg, H., 1978. Diffusion and relaxation in glassy polymer powders: 2. Separation of diffusion and relaxation parameters. *Polymer*, **19** 489–496.
[19] Sanopoulou, M. and Petropoulos, J., 1997. Sorption and longitudinal swelling kinetic behaviour in the system cellulose acetate-methanol. *Polymer*, **23** 5761–5768.
[20] Boom, J. and Sanopoulou, M., 2000. Interval sorption kinetics in the system poly(methyl methacrylate)-methylacetate. *Polymer*, **41** 8641–8648.
[21] Petropoulos, H., 1984. Interpretation of anomalous sorption kinetics in polymer-penetrant systems in terms of a time dependent solubility coefficient. *J. Pol. Sci., Polym. Phys. Ed.*, **22** 1885–1900.
[22] Doumenc, F., Guerrier, B., Allain, C., Dimos, V. and Sanopoulou, M., 2005. Solvent sorption in glassy polymer films - coupling between solvent diffusion and viscoelastic relaxation. ICCHMT, Fourth Int. Conf. on Computational Heat and Mass Transfer, Paris (Lavoisier).
[23] Vrentas, J., Duda, J. and Hou, A., 1984. Anomalous sorption in poly(ethyl methacrylate). *Journal of Applied Polymer Science*, **29** 399–406.
[24] Smith, M. and Peppas, N., 1985. Effect of the degree of crosslinking on penetrant transport in polystyrene. *Polymer*, **26** 569.

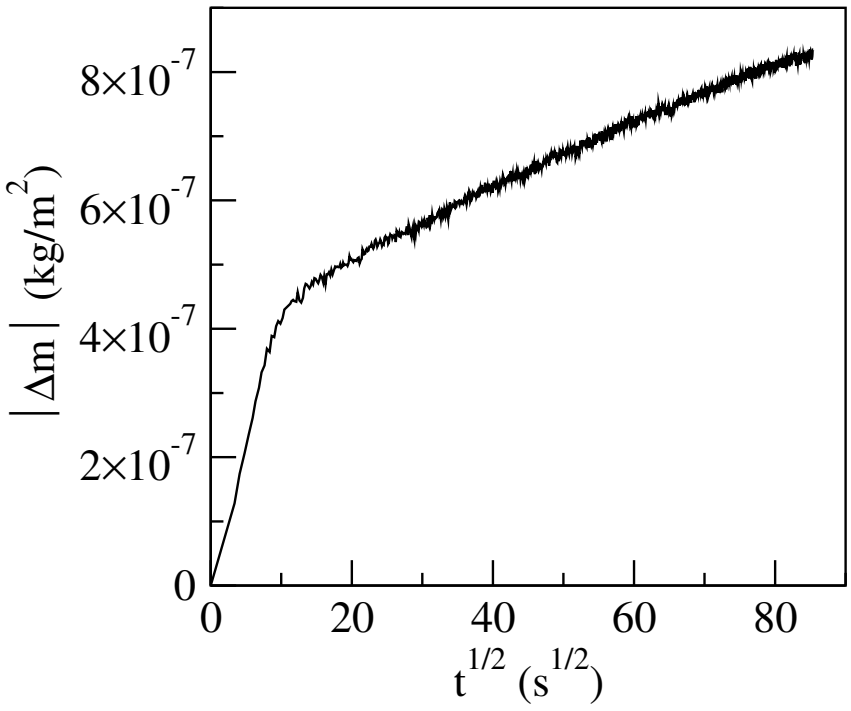

Figure 1. Experimental kinetics obtained for a decreasing pressure step (5.5 to 5.3 mbar) with a 65/35 PMMA/PnBMA copolymer. The ordinate is the absolute value of the mass variation per unit area.

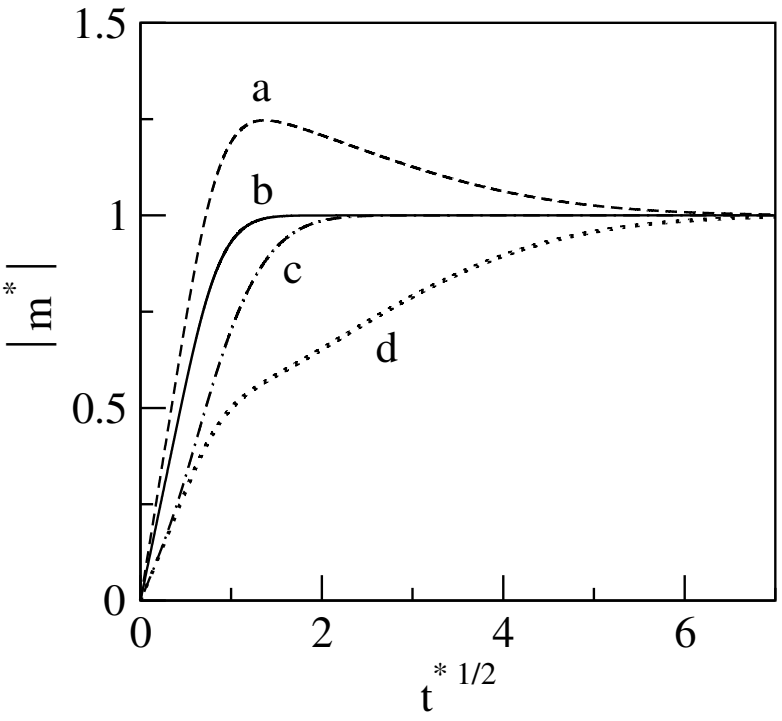

Figure 2. Model output for different values of Deb and R. From top to bottom: $Deb = 10$ and $R = 1.3$ (a), Fickian case (continuous line, b), $Deb = 1$ and $R = 0.5$ (c), $Deb = 10$ and $R = 0.5$ (d).

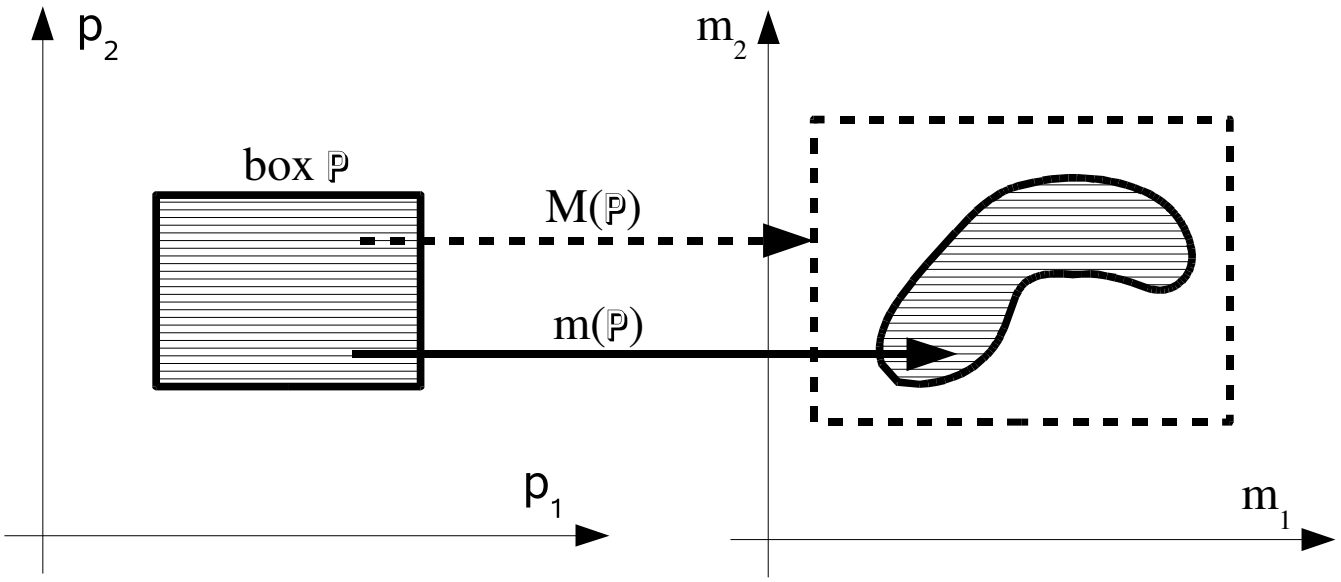

Figure 3. Schematic representation of the inclusion function.

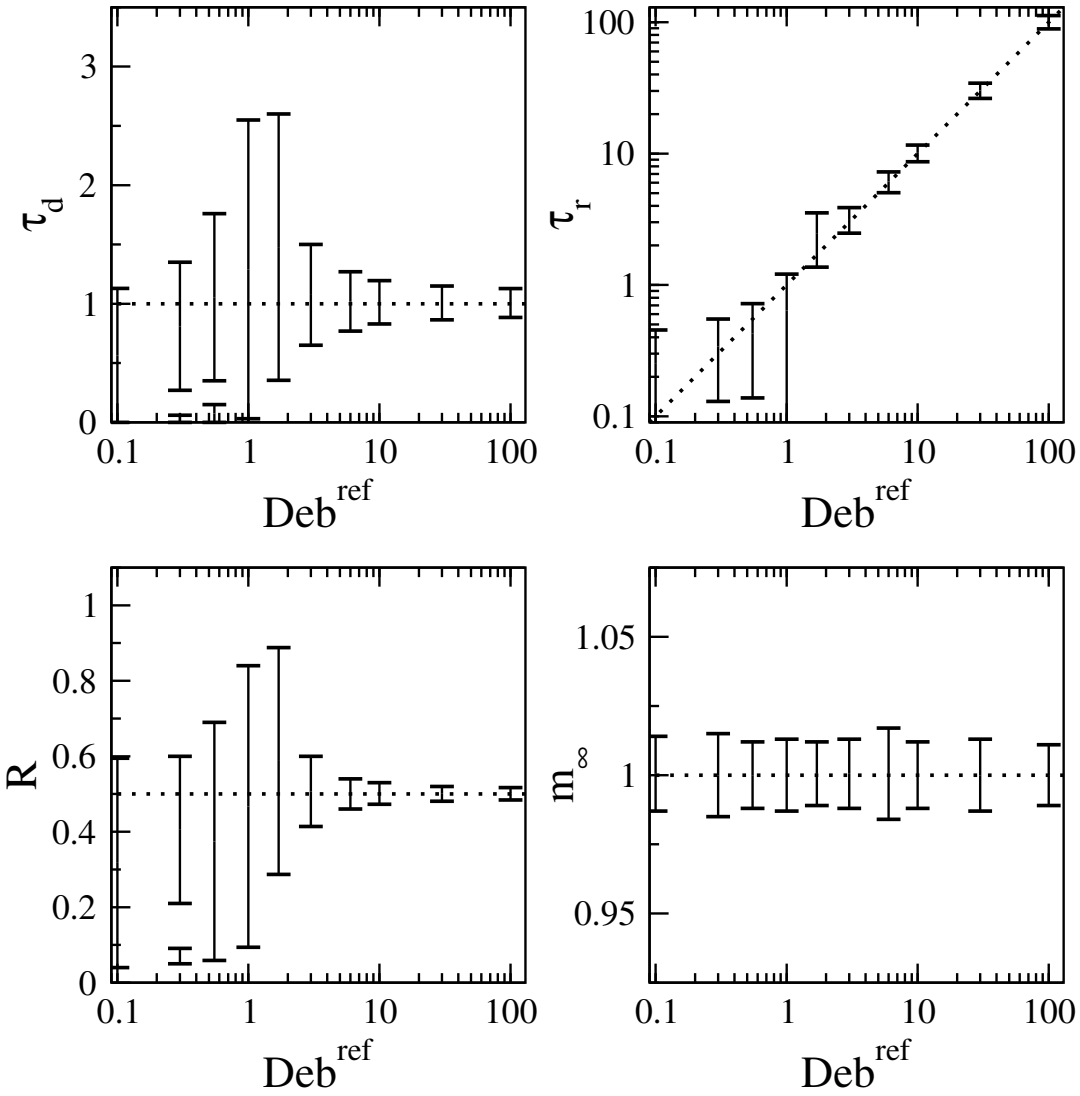

Figure 4. Influence of Deb^{ref}. Test case: $\tau_d^{ref} = 1$, $m_\infty^{ref} = 1$, $R^{ref} = 0.5$, large H, $\sigma = 0.01$ - 1D projection - The dotted line is the exact solution.

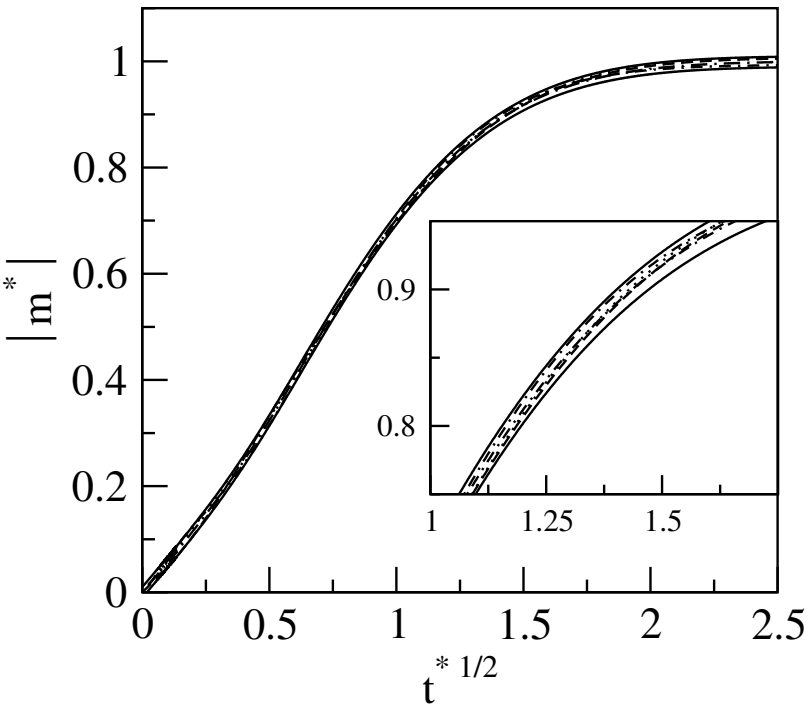

Figure 5. Test case: $\tau_d^{ref} = 1,\ \tau_r^{ref} = 1,\ R^{ref} = 0.5,\ m_\infty^{ref} = 1$. The two bounding curves $m_{exp} - \sigma$ and $m_{exp} + \sigma$ are continuous lines. Non continuous lines correspond to the reference kinetics m_{exp} and three estimated kinetics obtained with the following quadruplets: $\{\tau_d = 2.47,\ \tau_r = 0.089,\ R = 0.65,\ m_\infty = 1.007\}$ - $\{\tau_d = 0.042,\ \tau_r = 0.88,\ R = 0.11,\ m_\infty = 0.993\}$ - $\{\tau_d = 2.40,\ \tau_r = 0.25,\ R = 0.82,\ m_\infty = 1.007\}$.

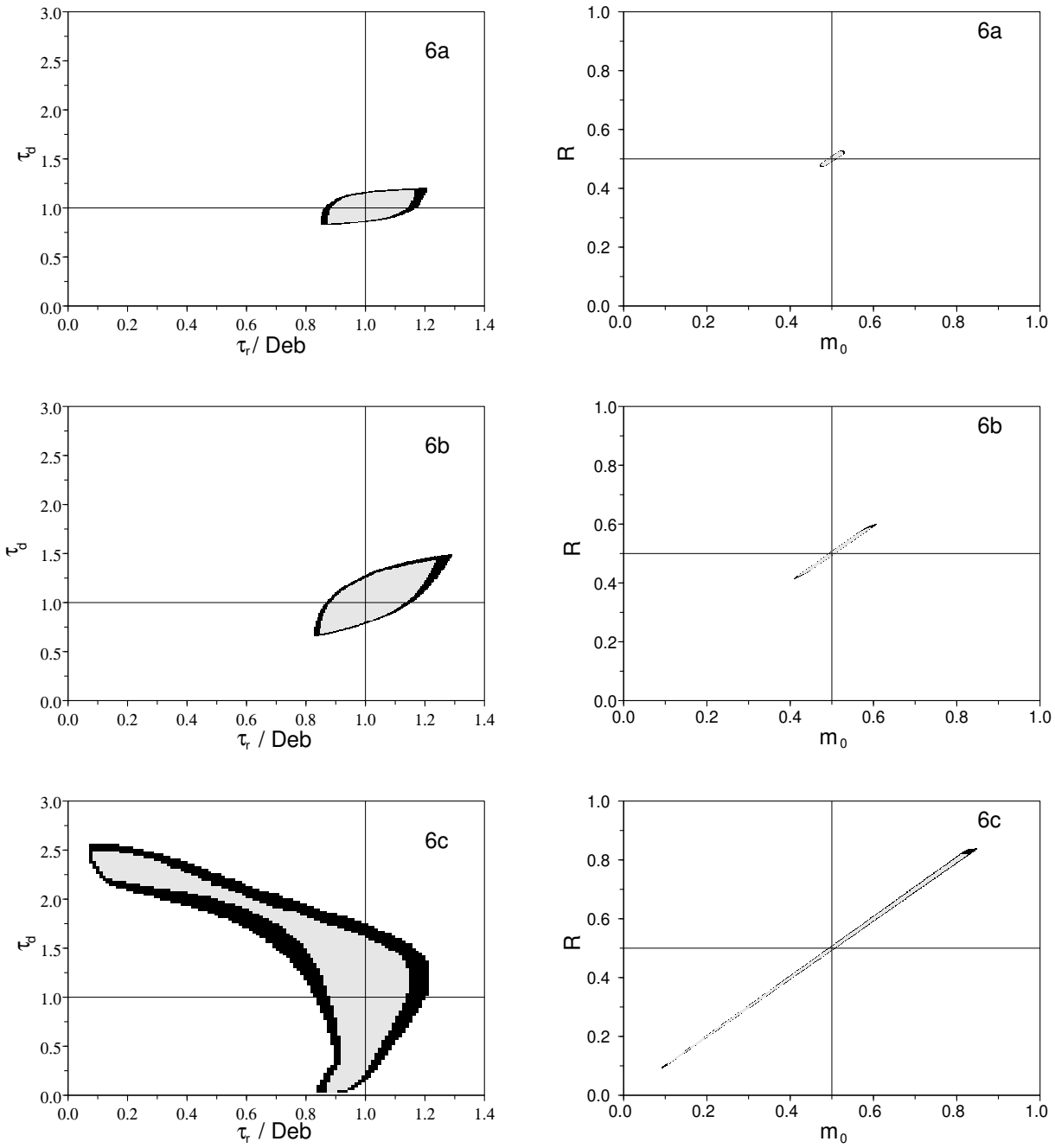

Figure 6. Influence of Deb^{ref}. Same test case as in Figure 4 - 2D projections: ' τ_r/Deb^{ref}-τ_d' space and 'm_0-R' space - Admissible domain (grey) and indeterminate domain (black) - (a) $Deb^{ref} = 10$, (b) $Deb^{ref} = 3$, (c) $Deb^{ref} = 1$.

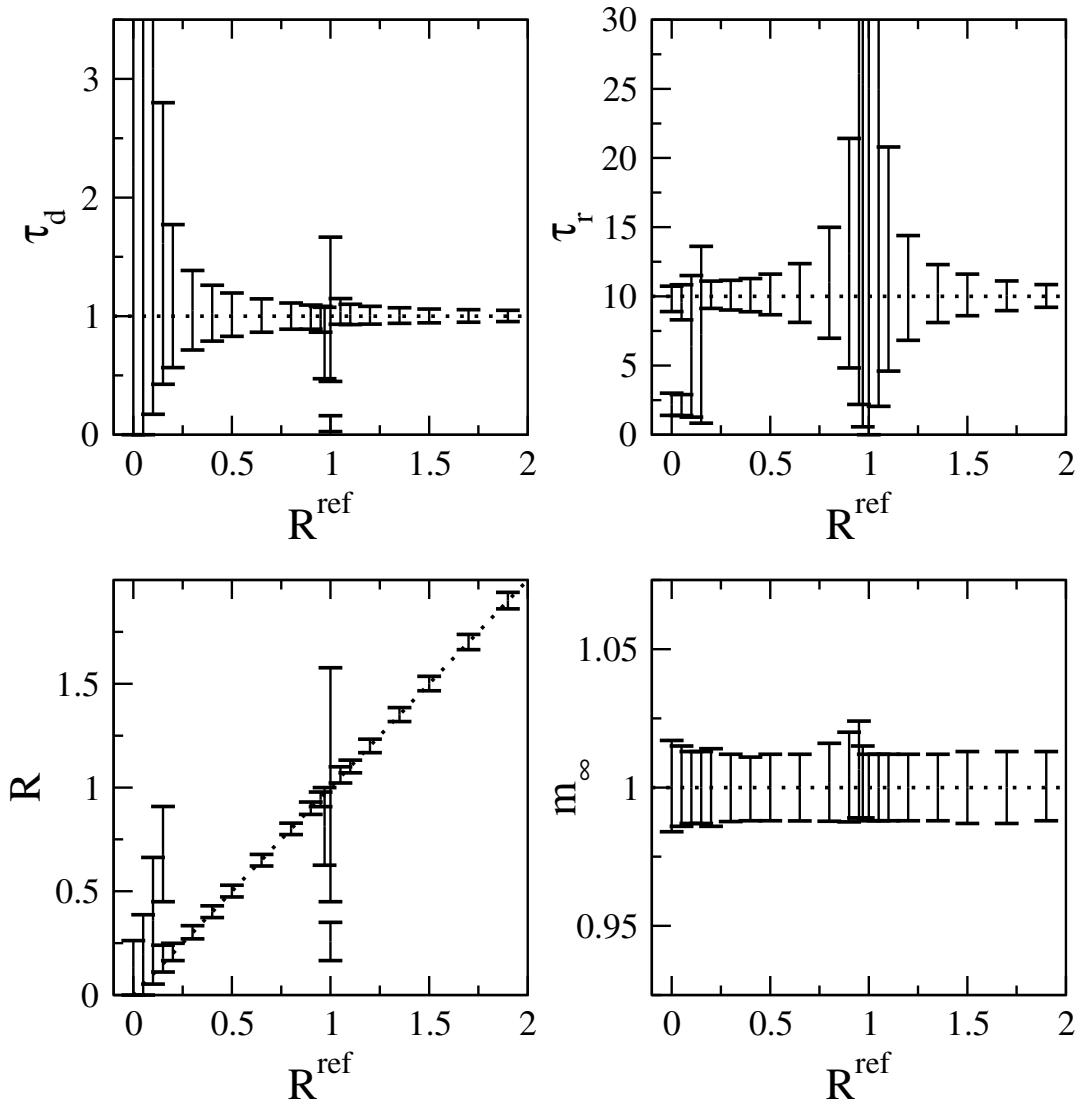

Figure 7. Influence of R^{ref}. Test case: $\tau_d^{ref} = 1$, $m_\infty^{ref} = 1$, $Deb^{ref} = 10$, large H, $\sigma = 0.01$ - 1D projection.

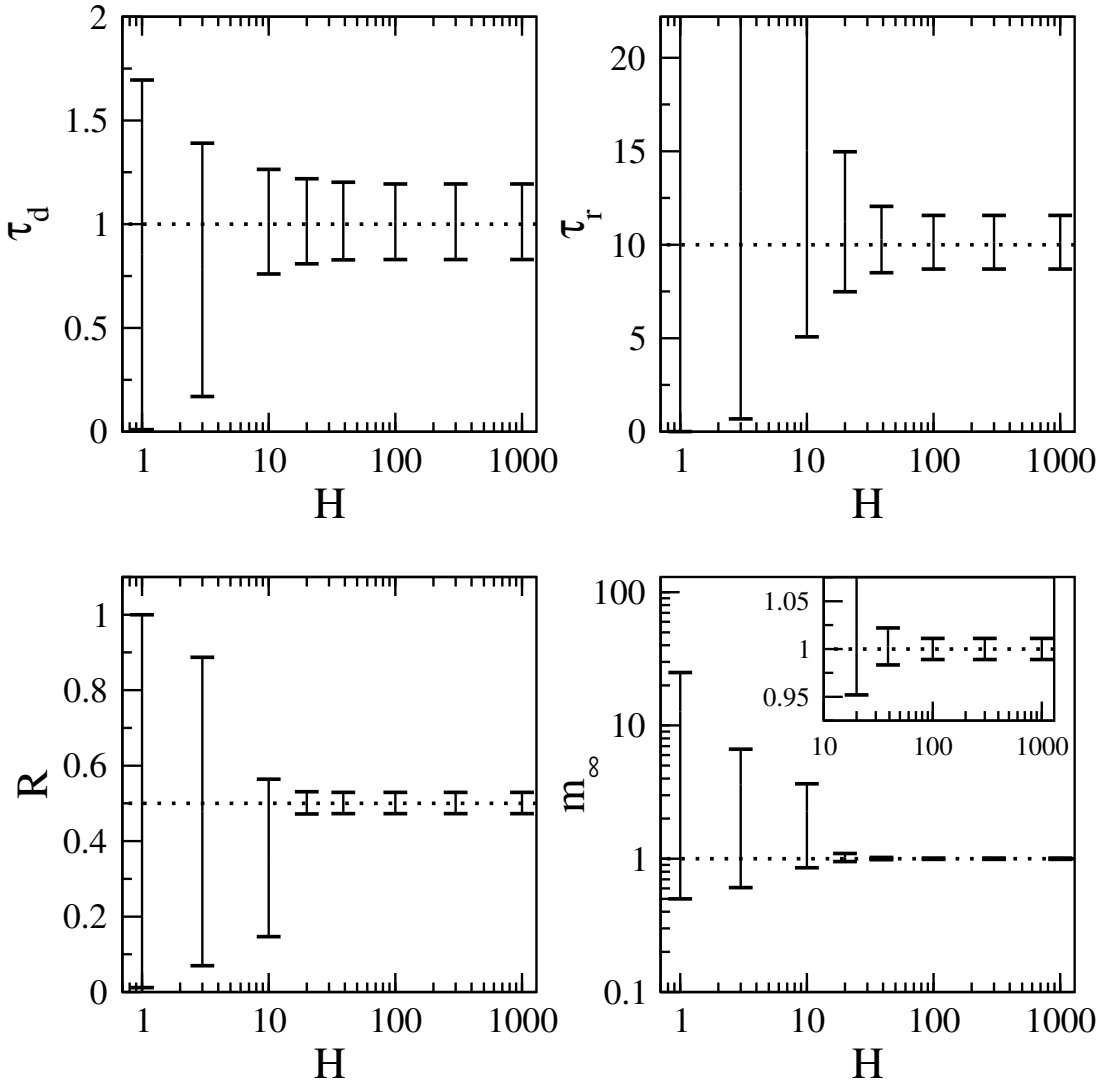

Figure 8. Influence of H. Test case: $\tau_d^{ref} = 1$, $m_\infty^{ref} = 1$, $Deb^{ref} = 10$, $R^{ref} = 0.5$, $\sigma = 0.01$ - 1D projection.

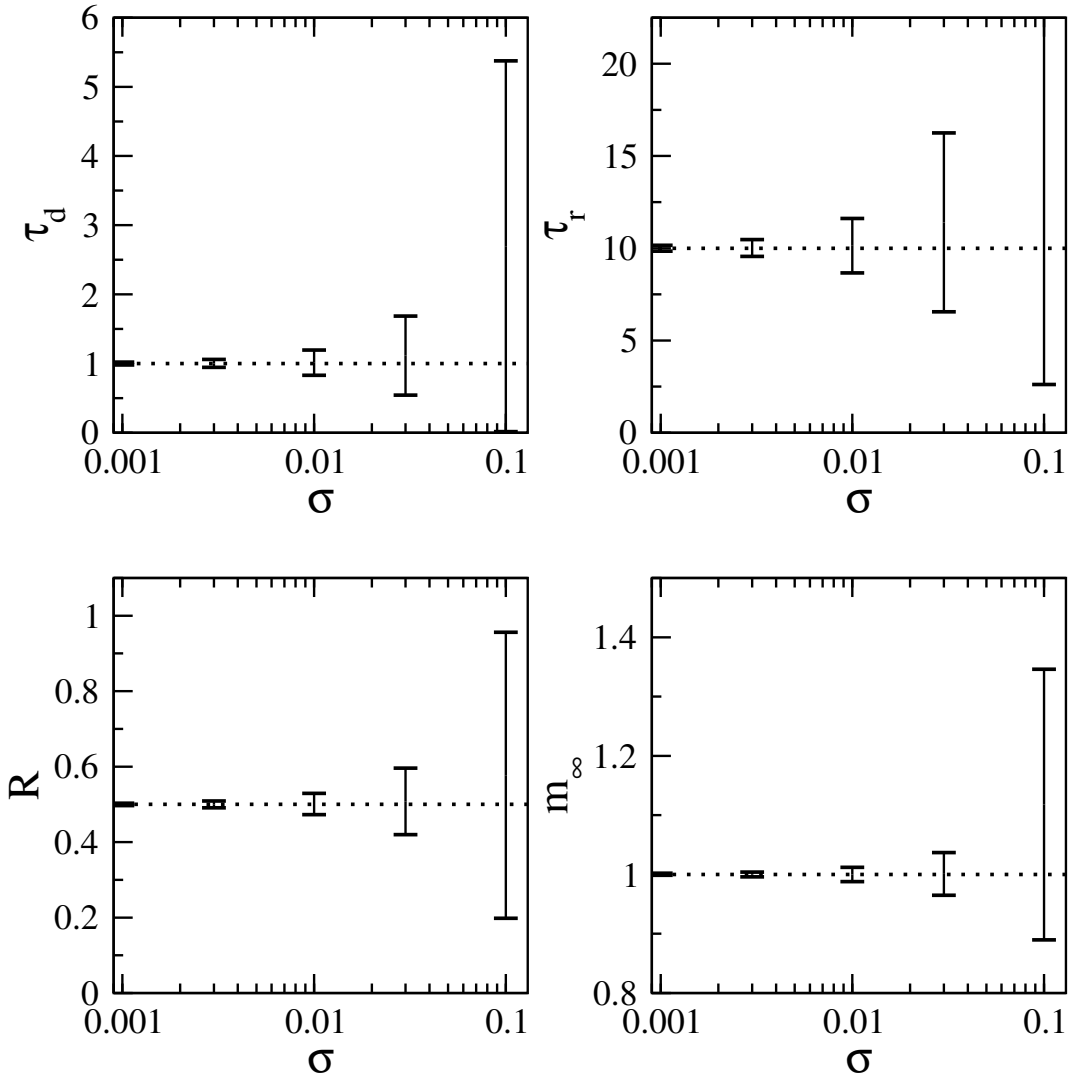

Figure 9. Influence of σ. Test case: $\tau_d^{ref} = 1$, $m_\infty^{ref} = 1$, $Deb^{ref} = 10$, $R^{ref} = 0.5$, large H, - 1D projection.

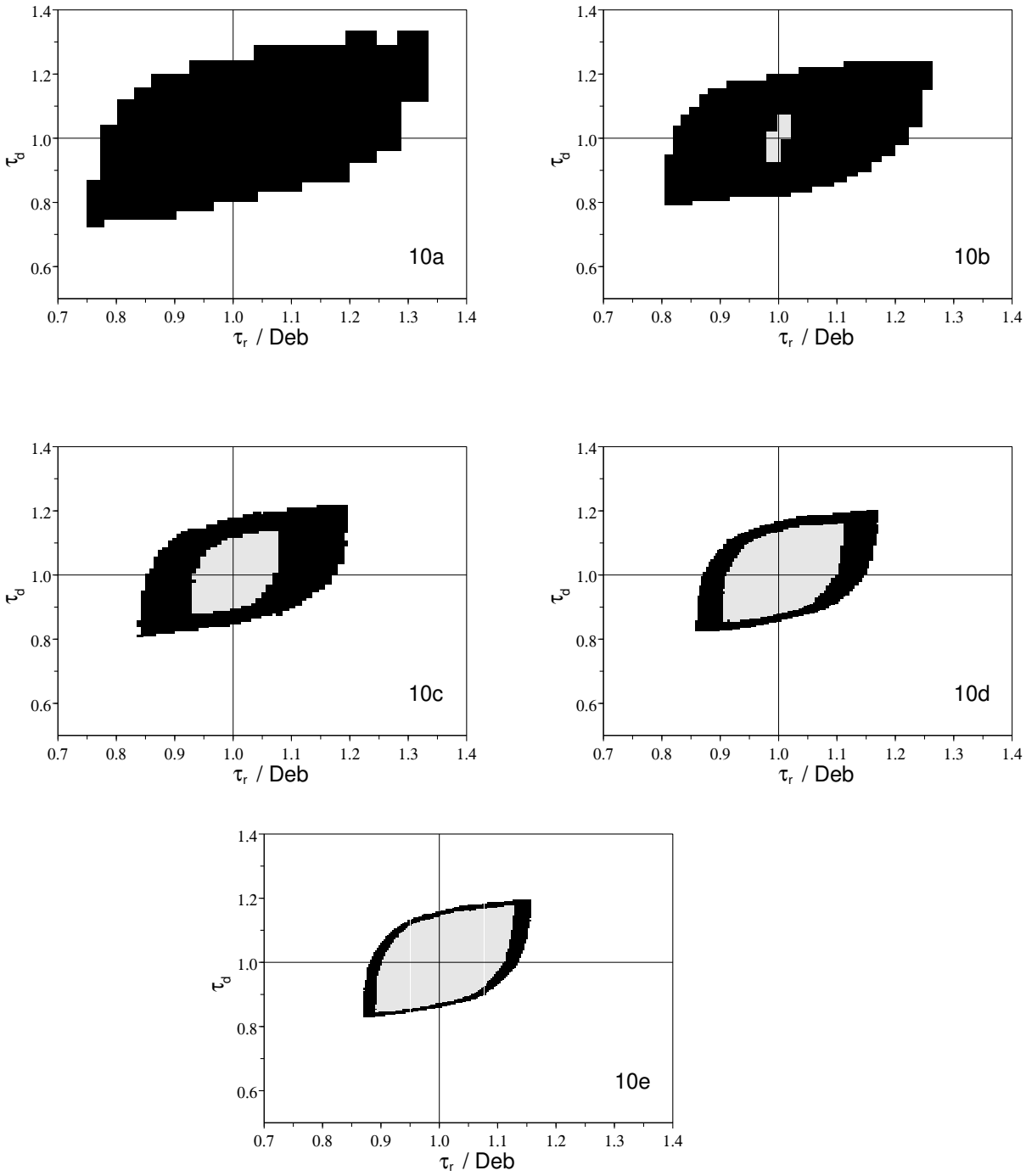

Figure 10. Partition in admissible domain (K_A, grey) and indeterminate domain (K_I, black) for different ε. Same test case as in Figure 4 - 2D projections: 'τ_r/Deb^{ref}-τ_d' space (a) $\varepsilon = 8 \times 10^{-3}$, (b) $\varepsilon = 4 \times 10^{-3}$, (c) $\varepsilon = 2 \times 10^{-3}$, (d) $\varepsilon = 10^{-3}$, (e) $\varepsilon = 5 \times 10^{-4}$.

Appendix A: Inclusion function

To determine the inclusion function needed in the set inversion analysis, let us consider the model described in section 2. The two boundary conditions are the flux at the bottom interface and the concentration at the top interface. The output is the mass uptake, $m(t)$, i.e. the integral of the concentration uptake on the film thickness. The state equation is given by equation (1). With the assumption of constant thickness and constant diffusion coefficient this model is linear. The output can be deduced from Laplace transform and is given by equation (5). This expression is however too complex to direct deduce the direction of variation of $m(t)$ with each parameter τ_d, τ_r, m_0 and R.

To overcome this difficulty, the output is expressed as the convolution product of the impulse response function and the input. The flux at the bottom being always equal to zero, one obtains:

$$m(t) = \int_0^t y(t^{'}) \times c(l, t - t^{'}) dt^{'} \tag{A1}$$

where $y(t)$ is the mass uptake when the input is a Dirac unit impulse, $\delta(t)$, and where $c(l, t)$ is given by equation (2).

$y(t)$ can be calculated by use of Laplace transform and is given by:

$$y(t) = 2 \times l \sum_{k=0}^{\infty} \frac{1}{\tau_d} exp\left[-k^{'2} t/\tau_d\right] \tag{A2}$$

where $k^{'} = (2k+1)\frac{\pi}{2}$. $y(t)$ is always positive; $c(l, t)$ is an increasing function of m_0 and a decreasing function of R and τ_r. Then, from equation (A1), the mass uptake $m(t)$ is also an increasing function of m_0 and a decreasing function of R and τ_r.

The derivative of $y(t)$ with respect to τ_d does not allow to conclude on the direction of variation of $m(t)$ with τ_d. To overcome this difficulty equation (A1) is integrated by parts, that leads to the following expression (where $Y(t)$ is the response to the Heaviside function H(t)):

$$m(t) = c_0 \times Y(t) - \int_0^t Y(t^{'}) \times \frac{d[c(l, t - t^{'})]}{dt^{'}} dt^{'} \tag{A3}$$

with

$$Y(t) = l \times \left(1 \ - 2 \sum_{k=0}^{\infty} \frac{1}{k'^2} \, exp\left[-k'^2 t/\tau_d \right] \right) \tag{A4}$$

Three cases have to be considered according to the value of R:

A.1 $R < 1$

When $R < 1$, the derivative $d[c(l, t - t')]/dt'$ is negative so that c_0 and $-d[c(l, t - t']/dt'$ are both positive. The derivative of $Y(t)$ with respect to τ_d being negative, $Y(t)$ is a decreasing function of τ_d and then the mass uptake $m(t)$ is also a decreasing function of τ_d if $R < 1$.

As a conclusion, when $R < 1$, the model output is a monotonic function of the four parameters τ_d, τ_r, m_0 and R: it is an increasing function of m_0 and a decreasing function of τ_d, τ_r and R. The model output for any quadruplet of a box is then included between the outputs m_{low} and m_{up} obtained by the quadruplets $\mathbf{p_{low}} = \{\tau_{d_{max}}, \tau_{r_{max}}, m_{0_{min}}, R_{max}\}$ and $\mathbf{p_{up}} = \{\tau_{d_{min}}, \tau_{r_{min}}, m_{0_{max}}, R_{min}\}$.

A.2 $R = 1$

When $R = 1$ the boundary condition is reduced to c_0 and the output does not depend on τ_r. It is an increasing function of m_0 and a decreasing function of τ_d so that the same values of m_{low} and m_{up} than previously can be used.

A.3 $R > 1$

When $R > 1$, c_0 and $-d[c(l, t - t')]/dt'$ have unlike signs. Due to the linearity of the model, it is possible to consider the two terms of the boundary condition independently and to divide the initial problem in two sub-problems.

The boundary condition of the first sub-problem is the first term of equation (2): $c_1(l, t) = c_0 \times H(t)$. The corresponding output $m_1(t) = c_0 \times Y(t)$ is a decreasing function of τ_d as $Y(t)$.

The boundary condition of the second sub-problem is the second term of equation (2): $c_2(l, t) = (c_\infty - c_0) \left\{ 1 - exp\left(-\frac{t}{\tau_r} \right) \right\}$. The derivative $d[c_2(l, t - t')]/dt'$ is positive when $R > 1$ so that the output of this sub-problem, $m_2(t)$, is an increasing function of τ_d.

To determine the inclusion function in the case $R > 1$, one overestimation of the output, m_{up}, can be obtained by adding the maximal value of the output

for each of the sub-problem:
$m_{up} = m_1(\tau_{d_{min}}, \tau_{r_{min}}, m_{0_{max}}, R_{min}) + m_2(\tau_{d_{max}}, \tau_{r_{min}}, m_{0_{max}}, R_{min})$

In the same way, one underestimation of the output, m_{low}, is obtained by adding the minimal value of the output for each of the sub-problem:
$m_{low} = m_1(\tau_{d_{max}}, \tau_{r_{max}}, m_{0_{min}}, R_{max}) + m_2(\tau_{d_{min}}, \tau_{r_{max}}, m_{0_{min}}, R_{max})$